Force-Sensorless Friction and Gravity Compensation for Robots

Santiago Morante, Juan G. Victores, Santiago Martínez, and Carlos Balaguer

Robotics Lab research group within the Department of Systems Engineering and Automation, Universidad Carlos III de Madrid (UC3M), smorante@ing.uc3m.es

Abstract. In this paper we present two controllers for robots that combine terms for the compensation of gravity forces, and the forces of friction of motors and gearboxes. The Low-Friction Zero-Gravity controller allows a guidance of the robot without effort, allowing small friction forces to reduce the free robot motion. It can serve to aid users providing kinesthetic demonstrations while programming by demonstration. In the present, kinesthetic demonstrations are usually aided by pure gravity compensators, and users must deal with friction. A Zero-Friction Zero-Gravity controller results in free movements, as if the robot were moving without friction or gravity influence. Ideally, only inertia drives the movements when zeroing the forces of friction and gravity. Coriolis and centrifugal forces are depreciated. The developed controllers have been tuned and tested for 1 DoF of a full-sized humanoid robot arm.

Keywords: robotics, control, dynamics, friction, force, humanoid

1 Introduction

Most robots are hard and heavy. They are built with metallic mechanical links and electric/hydraulic motors attached to heavy gearboxes that introduce high frictions. This fact makes it very difficult to physically interact with the robot. With the advent of paradigms such as Programming by Demonstration (PbD) [1], where physical movements are used to program the robot, there has been an increasing necessity to improve the existing physical interaction mechanisms.

We have developed two different types of controllers for robots which combine gravity compensation and motor friction compensation. Our motivation is to study new forms of physical human-robot interaction. In kinesthetic teaching, a popular choice in PbD, the robot's motors are set to a passive mode where each limb can be driven by the human demonstrator [2]. Some authors suggest that kinesthetic demonstrations are more intuitive for naive users, but that this fact changes when facing with high degree of freedom (DoF) robots [3]. They present an alternative, called keyframe demonstration, where key positions of the task are recorded, while the intermediate movements are interpolated. For instance, Baxter robot uses this technique of recording frames to be programmed, aided by gravity compensation [4]. While gravity compensation is useful for providing kinesthesic demonstrations, one of our controllers, called Low-Friction

Zero-Gravity controller (LFZG) adds an additional friction compensation term for aiding keyframe demonstration. We aim to create even simpler interactions with robots, as this controller makes the robot move in the direction indicated by small forces applied, eventually stopping. Additionally, our approach does not require torque or force sensors to be implemented. The second developed controller, formally Zero-Friction Zero-Gravity controller (ZFZG), makes the robot move similarly as if it were floating in space. As the forces that make the robot reduce its motion (mainly gravity and friction) are compensated, the final output is the free movement of the robot, driven by inertia.

2 State of the Art

The main fields of study of this work are related with friction and gravity compensation. Only selected works will be mentioned, as the literature in friction compensation in robots is extensive. A review can be found in [5].

On one side, friction is described as the resistance of motion of two contacting sliding surfaces [5]. To measure friction accurately is extremely difficult. Exact models of friction do not exist, and instead approximations obtained through experiments are used (Coulomb, viscous friction, Stribeck, Dahl, LuGre, Leuven, etc.). No specific model has proven better than others [6]. Canudas et al. [7] focused on modeling non-linear effects of friction in DC motor drives. They combine a linear model for viscous friction with a parameter estimation algorithm, which recalculates linear model parameters in a feedback loop to reduce the error in velocity commands. Some methods for friction identification in robotics consider elements in isolation, or do not consider mechanical limitations [8][9]. A low-velocity approach allows obtaining friction models depreciating inertia in [10]. As modeling motor frictions involves non-linearities (Stribeck effect, hysteresis, pre-sliding displacement, etc.), some authors [11] have delegated this problem to learning algorithms such as Neural Networks. Gearboxes also have high frictions, and additionally increase motor frictions from the link's point of view (due to the reduction factor). The most popular gearboxes in humanoid robotic platforms are Harmonic Drives, because of their compactness and reduction factor. Authors [12] have tried to model Harmonic Drives' frictions, finding similar problems of non-linearities as those of the motor case. Regarding humanoid robots, in [13] they identify friction parameters on an iCub robot, aided by 6-axis force/torque sensors.

On the other side, gravity compensation is computed using the dynamic model of the robot. By analyzing the kinematic configuration and the masses of links and motors, it is possible to calculate the influence of gravity in each motor, and compute the torque value necessary to compensate it. In [14] they compensate gravity by projecting gravity forces on each joint of a robot arm. First, they translate all joint coordinates to the base frame. Then, they project on each joint, the torque generates by gravity forces on the rest of links and motors. This method is a simple and methodical procedure to compensate gravity in rigid links. In classical literature, the inclusion of a gravity compensation term in robot

manipulation control schemes was used for improving a PD position control [15]. Including gravity compensation performed as well as a full feedforward controller with full inertial terms. Another work [16] aimed at estimating and compensating gravity and friction forces in the context of improving the position error in robot manipulators. However, the possibility of simulating free movements was not studied.

3 Theoretical Foundations

The design of our controllers is related with the fundamental laws of dynamics for serial rigid multibody systems. We consider the Euler-Lagrange equations of motion of multibody rigid links in the robot joint space as:

$$B(q)\ddot{q} + C(q,\dot{q})\dot{q} + F_v\dot{q} + F_s\,\mathrm{sgn}(\dot{q}) + g(q) = u + \tau_{ext} \tag{1}$$

Where B is the inertia matrix, C represents the centrifugal and Coriolis forces, $F_v\dot{q}$ is the viscous friction torque, $F_s\,\mathrm{sgn}(\dot{q})$ is the Coulomb friction torque, F_v is the matrix of viscous friction coefficients, $g(q)$ is the gravity term, u is the actuation torque, and finally τ_{ext} is the torque originated by external forces. An ideal friction and gravity compensator could be expressed as a u with the following form:

$$u = F_v\dot{q} + F_s\,\mathrm{sgn}(\dot{q}) + g(q) \tag{2}$$

Due to the low speeds applied in robotics, the Coriolis and centrifugal forces C are negligible. Substituting (2) in (1):

$$B(q)\ddot{q} = \tau_{ext} \tag{3}$$

Which means that the mechanism would offer a resistance to external forces (e.g. pushing or pulling) equivalent only to its inertia. When applied to a robotic system, this controller would make the whole mechanism behave as if it were in free movement. Our controllers combine friction and gravity compensation terms to provide new forms of physical interaction with robots. Let us formally describe the equations governing the controllers. Let $g(q)$ be the term of gravity compensation, with q as the actual joint configuration. Let $\tau_f(q,\dot{q})$ be the term of friction compensation, where $\dot{q}$ is the joint angular velocity. Then, a generic friction and gravity compensation controller can be expressed as:

$$u = g(q) + \tau_f(q,\dot{q}) \tag{4}$$

A block scheme of this generic friction and gravity compensation controller can be seen on Fig. 1. Let us now describe how the gravity and friction compensation terms can be determined.

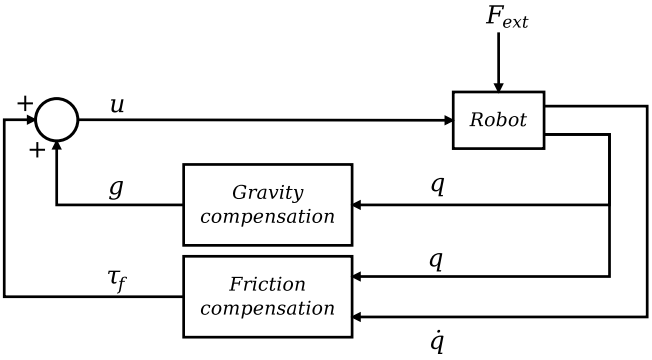

Fig. 1. Block scheme of friction and gravity compensation. In this type of control, there is no external reference, the robotic system is moved by the external perturbations caused by the user.

3.1 Gravity Compensation

The potential energy of a robot, assuming rigid links and punctual masses, can be defined as [17]:

$$U = \sum_{i=1}^{n} (U_{l_i} + U_{m_i}) \tag{5}$$

Where U_{l_i} is the sum of potential energy contributions of each link, U_{m_i} is the contribution of each motor, and i is an index for each link or motor. The first term U_{l_i} is defined as:

$$U_{l_i} = -m_{l_i} g_0^T p_{l_i} \tag{6}$$

Where m_{l_i} is the mass of the center of masses of link i, g_0 is the gravity vector expressed in base frame (e.g. $g_0 = [0 \quad 0 \quad -9.81]^T$), and p_{l_i} is the set of coordinates of the center of masses of link i expressed in the base frame. Similarly, the motor contributions U_{m_i} are defined as:

$$U_{m_i} = -m_{m_i} g_0^T p_{m_i} \tag{7}$$

Substituting (6) and (7) in (5), U becomes:

$$U = -\sum_{i=1}^{n} (m_{l_i} g_0^T p_{l_i} + m_{m_i} g_0^T p_{m_i}) \tag{8}$$

Where p_{l_i} and p_{m_i} depend on the joint configuration q. The torque $g(q)$ exerted by gravity can be computed as [18]:

$$g(q) = \frac{\partial U}{\partial q} \tag{9}$$

And is thus the torque required for gravity compensation. In the real world, determining the influence of each element in the potential energy equation is a non-trivial issue. For instance, the distinction between motor and link mass contribution is blurry, as the mass contribution between motors includes the parts of the motors located between the axes of rotation. This is the reason why we will use a simplified dynamic model of U. In this simplified model, the terms of link and motor contributions are mixed, and their masses are concentrated in the intermediate point between each pair of axes of rotation. This dynamic model is commonly used in humanoid robot research, and is usually called 'mass concentrated model'.

3.2 Friction Compensation

The static friction forces, $F_v\dot{q}+F_s\,\mathrm{sgn}(\dot{q})$, from (1) can be compacted into a joint friction term, $\tau_{fj}(\dot{q})$. It can be computed with a model-based identification procedure inspired by [19]. Among the available friction models, they have assumed the one including Coulomb friction (initial opposing torque) and viscous friction (friction dependent on velocity). Their aim is to model the friction of an electric motor. The motion of an electric motor can be described as:

$$\tau_m(t) - \tau_{fm}(\dot{\theta}) = J\ddot{\theta} \tag{10}$$

Where τ_m is the motor torque, $\tau_{fm}(\dot{\theta})$ is the motor friction torque, $\ddot{\theta}$ is the motor angular acceleration and J is the inertia of the motor. If the angular velocity $\dot{\theta}$ is stabilized, then $\ddot{\theta} = 0$, so the torque of the motor is used exclusively to compensate the friction:

$$\tau_m(t) = \tau_{fm}(\dot{\theta}) \tag{11}$$

Measuring the different velocities where the motor stabilizes for several torques applied, the stabilized velocities for these different torques can be plotted. The friction model selected by [19] becomes a piecewise linear model:

$$\tau_{fm}(\dot{q}) = \begin{cases} \alpha_1\dot{\theta} + \beta_1 : \ \dot{\theta} > 0 \\ \alpha_2\dot{\theta} - \beta_2 : \ \dot{\theta} < 0 \end{cases} \tag{12}$$

Where model parameters α and β are obtained by linear regression on the plot (Fig. 2).

In the original procedure, they measure the motor velocity $\dot{\theta}$ in isolation. In our proposed identification procedure, we measure the velocity $\dot{q}$ with the motor within the robot, including the gearboxes and the mechanical structure. Modeling each part independently (motor, gearbox, structure, construction) would result in intractable combinations of models to be evaluated and coordinated, specially for many DoF. Our assumptions are the following:

- We use joint velocity $\dot{q}$ instead of motor velocity $\dot{\theta}$. The joint friction model selected becomes the following piecewise linear model:

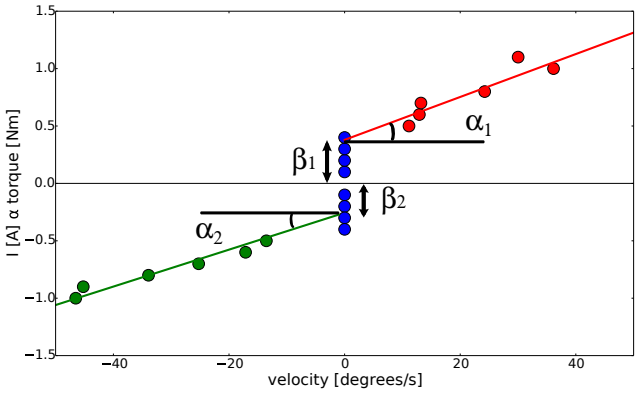

Fig. 2. This friction model includes Coulomb friction and viscous friction. The variables α and β represent the parameters of the linear model assumed.

$$\tau_{fj}(\dot{q}) = \begin{cases} \alpha_1 \dot{q} + \beta_1 : & \dot{q} > 0 \\ \alpha_2 \dot{q} - \beta_2 : & \dot{q} < 0 \end{cases} \tag{13}$$

Where $\tau_{fj}(\dot{q})$ is the torque necessary to compensate the friction generated in function of the joint angular velocity $\dot{q}$.

- We assume that the motors have a symmetrical behavior, they oppose to movement in both directions with the same strength. Therefore, $\alpha_1 = \alpha_2$ and $\beta_1 = \beta_2$.
- When applying constant torques, we limit the time given for velocity stabilization due to the mechanical constraints of the robot joints.
- As we have to deal with gravity forces, which may influence friction, we add an additional term when opposing gravity.

Robot joints have mechanical constraints, so there is a limit in the time the joint velocity can be recorded. This time may not be enough for the velocity to stabilize. In these cases, the velocity achieved before reaching the joint limit must be used instead of the stabilized velocity. This causes a steeper slope of the posterior linear regression. The final parameters of the linear regression should be further adjusted in these cases.

As stated in our final assumption, we add a term in addition to $\tau_{fj}(\dot{q})$. We assume that an additional mechanical friction is generated in the motor axle and gearbox due to gravity. This is the reason why we have added a term τ_{fg} dependent on the joint position and the velocity:

$$\tau_{fg} = f(q, \dot{q}) \tag{14}$$

The term $\tau_{fg}(q, \dot{q})$ is purely experimental, as it depends on the mechanical design and construction of the robot. In our model, we only add this term when the gravity opposes the direction movement of the arm. To see whether the

gravity is in favor or against this movement, the variation of the potential energy U can be used. When $\Delta U > 0$, the movement is against gravity. The final friction compensator can be expressed as:

$$\tau_f(q, \dot{q}) = \begin{cases} \tau_{fj}(\dot{q}) + \tau_{fg}(q, \dot{q}) : & \Delta U > 0 \\ \tau_{fj}(\dot{q}) & : \ \Delta U < 0 \end{cases} \tag{15}$$

3.3 Friction and Gravity Compensation Controllers

Different applications may require different behaviors of the robot. Hence, two controllers have been derived from the generic friction and gravity compensation controller (4).

Low-Friction Zero-Gravity controller (LFZG) This controller can improve the physical interaction with robots. In this controller, a new parameter ξ has been incorporated. This parameter attenuates the influence of the friction compensation on the system. Introducing ξ in the controller, it becomes:

$$u = g(q) + \xi \tau_f(q, \dot{q}) \tag{16}$$

By setting $0 < \xi < 1$, this controller allows the robot to move easily, without effort, but eventually stopping due to the low friction. This controller can be useful in paradigms such as keyframe demonstration and PbD, where there is a direct physical contact with the robot. For instance, when aiming to record a task using keyframe demonstration, different robot configurations must be recorded. In many cases, a demonstrator may have to use both hands to move a single robot joint, due to its individual friction. Therefore, in robots with many DoF, it can be difficult to physically move the robot between the different desired configurations. Using our controller, one has to simply push the robot in the desired direction, and stop it when desired. The attenuated friction serves as an aid for stopping at the desired target keyframes.

Zero-Friction Zero-Gravity controller (ZFZG) This controller, when applied to all joints, ideally makes the robot move as if only the external dynamic forces and inertia would modify the motion. To achieve this behavior, we can use the generic friction and gravity compensation controller (4):

$$u = g(q) + \tau_f(q, \dot{q}) \tag{17}$$

A robotic platform using this control could be employed to test how devices would behave in complete absence of friction and gravity.

4 Experiments

The experiments have been performed using the arm of the humanoid robot Teo [20]. A single 1 DoF robot joint was tested, in order to avoid the high-dimensionality and coupling effects of many DoF (similarly to [21]).The humanoid robot joint used was the robot's left shoulder, which is moved by a Maxon brushless EC flat motor. It has a torque constant of 0.0706 Nm/A. The motor driver has an internal current loop with a PI regulator, with constant $K_p = 0$ and $K_i = 0.1651$. The gearbox is a Harmonic Drive CSD-25 with a reduction factor of 160. Joint position is measured using an optical relative encoder attached to the motor. Velocity is obtained by numerical differentiation of the position signal.

The robot arm weight m is 4.446 kg (including hand and electronics), and it has a length L of 0.82 m. The control algorithms were implemented in C language. The gravity compensation term of the control was computed as the torque caused by the arm modeled as a punctual mass at its center of gravity. Considering h as the height of the center of gravity with respect to its lowest position, being a single joint, this term is trivial to be calculated. Assuming q_1 as the angle between the arm and the trunk, the potential energy of a mass situated at $L/2$ from the shoulder is:

$$U = mg_0\, h = mg_0(L/2)(1 - cos(q_1)) \tag{18}$$

Then, the gravity torque term is:

$$g(q_1) = \frac{\partial U}{\partial q_1} = mg_0(L/2)\sin(q_1) \tag{19}$$

The friction compensation term was determined by the procedure indicated in previous sections. When high torques are applied to the motor, leading to high velocities, the motor is not able to stabilize its velocity before reaching the mechanical limit. This results in a steeper slope on the posterior regression. This effect can be seen in the shortest curves in Fig. 3. Fourteen different constant motor torques were tested, including both movements against and in favor of gravity, ranging between -0.0706 Nm and 0.0706 Nm (from -1 A to 1 A). In our case, positive velocities go against gravity, and negative velocities are in favor of gravity. A summary of the process of friction identification for the joint can be seen first on Fig. 3, where the stability velocities are measured. Fig. 4 depicts the performed linear regressions.

The linear regressions obtained without manual tunning resulted in:

$$\tau_f(\dot{q_1}) = \begin{cases} 0.009\,\dot{q_1} + 0.490: & \Delta U > 0 \\ 0.005\,\dot{q_1} - 0.586: & \Delta U < 0 \end{cases} \tag{20}$$

A posterior manual adjustment of these linear regression parameters resulted in:

$$\tau_f(\dot{q_1}) = \begin{cases} 0.006\,\dot{q_1} + 0.4: & \Delta U > 0 \\ 0.001\,\dot{q_1} - 0.7: & \Delta U < 0 \end{cases} \tag{21}$$

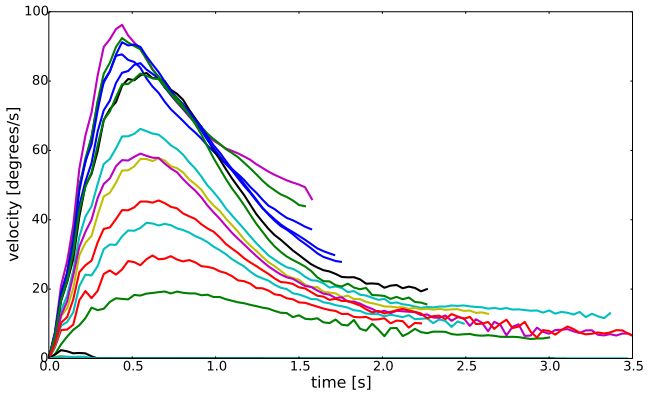

Fig. 3. Velocity vs. time curves, with constant torque applied in each curve. There is a proportional linear dependence between current in the motor and torque applied.

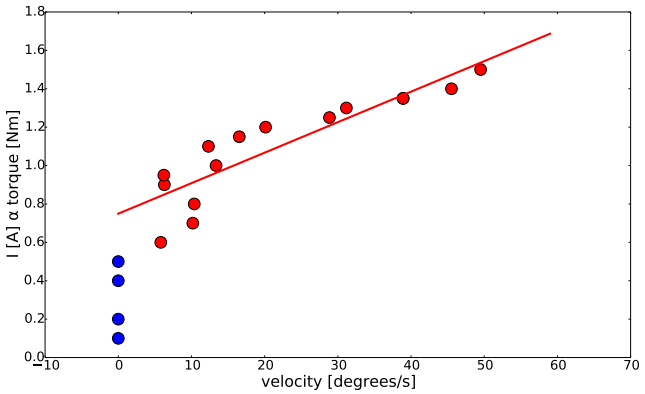

Fig. 4. Stabilization velocity vs. the torque applied. The Coulomb friction (blue) and the viscous friction (red) can be seen. The same procedure is applied for negative velocities.

To adjust to a symmetric joint friction model, either of the equations may be selected to fix the parameters of the model. Here, we have used the parameters of $\Delta U < 0$ case of (21), resulting in the joint friction term τ_{fj} of the controller:

$$\tau_{fj}(\dot{q_1}) = \begin{cases} 0.001\,\dot{q_1} + 0.7: & \Delta U > 0 \\ 0.001\,\dot{q_1} - 0.7: & \Delta U < 0 \end{cases} \tag{22}$$

All other frictions will be considered part of the gravity friction term τ_{fg}. The position-dependent parameter of τ_{fg} was experimentally adjusted to $0.0025\,q_1$. The final expression of τ_{fg} is computed as (21) minus (22) plus the position-dependent parameter τ_{fg}.

$$\tau_{fg}(q_1, \dot{q_1}) = 0.005\,\dot{q_1} + 0.0025\,q_1 - 0.3 \tag{23}$$

The compensators were evaluated activating the ZFZG controller. A well designed Zero-Friction Zero-Gravity controller would maintain constant, or tightly bounded, velocities in absence of external perturbations (beyond the one initiating the movement). To test whether these conditions are applicable to our system, several interactions with the arm were performed. A single push was given to the arm, letting it move freely while recording its velocities. This experiment was repeated while pushing the robot arm with different forces. Several velocity profiles for different pushes can be seen on Fig. 5.

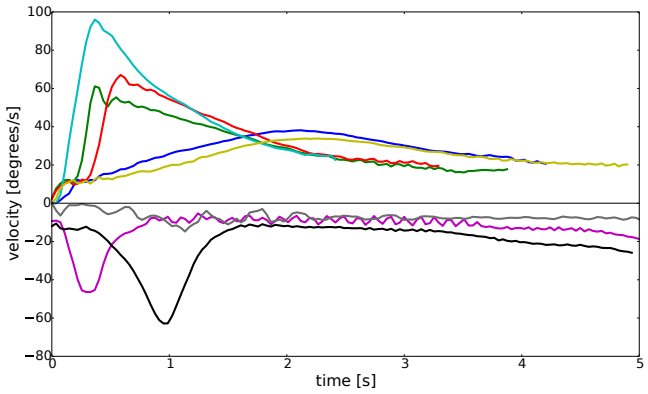

Fig. 5. Velocity profiles for several initial 'pushes' with the Zero-Friction Zero-Gravity controller (ZFZG).

Curves reaching higher peak values in the figure represent larger forces exerted by the human. The peak of each curve roughly represents the instant where the robot arm is let free. An example of one of these interactions using the ZFZG controller can be seen in Fig. 6.

Results from Fig. 5 showed that the combination of friction compensation and gravity compensation was successful at maintaining bounded velocities in ab-

Fig. 6. Sequence of the movement of the robot arm using a Zero-Friction Zero-Gravity controller. When the user pushes the arm, it moves freely in the direction of the applied force.

sence of external perturbations for velocities below 30-35 degrees/s. Results also show that the friction model is not adequate for velocities above 30-35 degrees/s. For instance, the light blue and purple curves do not maintain their values after their peaks. This could be explained because of the unmodeled non-linearities of the friction function at these velocities. A video of the implementation was shown in Humanoids 2014 conference [22], and can be seen online[1].

Our linear friction model may look simplistic, as each part in the mechanism includes its own non-linearities. However, it accounts for physical components (such as gearboxes and joint limits) that are found in robotic systems. Ultimately, the controllers are able to manifest the friction and gravity compensation expected behavior for the tested robotic joint. Our efforts are directed to implement these control algorithms in our full humanoid robot.

5 Conclusions

In this paper, the authors have presented a new set of controllers for robots which aim at compensation of static friction and gravity. The experiments show, in general, an acceptable performance of the ZFZG controller tested. More accurate friction models and identification procedures could lead to improved controller behaviors under high joint velocity conditions, and would also aid in maintaining the stability of low velocities. We also consider using different dynamic robot models (pendulum-like models, or even the complete dynamic model).

With the potential increase in complexity of the complete humanoid robot model, we consider using machine learning algorithms which lighten the efforts necessary to obtain a reliable friction and gravity compensation. They could also capture the non-linearities present in the system.

Acknowledgments

This work was supported by RoboCity2030-III-CM project (S2013/MIT-2748), funded by Programas de Actividades I+D in Comunidad de Madrid and EU.

[1] `http://dai.ly/x2vjrfs`

References

1. Sylvain Calinon, Florent D'halluin, Eric L Sauser, Darwin G Caldwell, and Aude G Billard. Learning and reproduction of gestures by imitation. *IEEE Robotics & Automation Magazine*, 17(2):44–54, 2010.
2. Aude G Billard, Sylvain Calinon, and Florent Guenter. Discriminative and adaptive imitation in uni-manual and bi-manual tasks. *Robotics and Autonomous Systems*, 54(5):370–384, 2006.
3. Baris Akgun, Maya Cakmak, Jae Wook Yoo, and Andrea Lockerd Thomaz. Trajectories and keyframes for kinesthetic teaching: A human-robot interaction perspective. In *Proceedings of the seventh annual ACM/IEEE international conference on Human-Robot Interaction*, pages 391–398. ACM, 2012.
4. Erico Guizzo and Evan Ackerman. The rise of the robot worker. *Spectrum, IEEE*, 49(10):34–41, 2012.
5. Henrik Olsson, Karl J Åström, Carlos Canudas de Wit, Magnus Gäfvert, and Pablo Lischinsky. Friction models and friction compensation. *European journal of control*, 4(3):176–195, 1998.
6. Basilio Bona and Marina Indri. Friction compensation in robotics: an overview. In *IEEE Conference on Decision and Control, 2005 and 2005 European Control Conference. CDC-ECC'05. 44th*, pages 4360–4367. IEEE, 2005.
7. Carlos Canudas, K Astrom, and Konrad Braun. Adaptive friction compensation in dc-motor drives. *IEEE Journal of Robotics and Automation*, 3(6):681–685, 1987.
8. Dragan Kostic, Bram de Jager, Maarten Steinbuch, and Ron Hensen. Modeling and identification for high-performance robot control: an rrr-robotic arm case study. *IEEE Transactions on Control Systems Technology*, 12(6):904–919, 2004.
9. Evangelos G Papadopoulos and Georgios C Chasparis. Analysis and model-based control of servomechanisms with friction. *Journal of dynamic systems, measurement, and control*, 126(4):911–915, 2004.
10. Mehrdad R Kermani, Mathew Wong, Rajnikant V Patel, Mehrdad Moallem, and Mile Ostojic. Friction compensation in low and high-reversal-velocity manipulators. In *Proceedings on IEEE International Conference on Robotics and Automation, 2004. ICRA'04.*, volume 5, pages 4320–4325. IEEE, 2004.
11. Jing Na, Qiang Chen, Xuemei Ren, and Yu Guo. Adaptive prescribed performance motion control of servo mechanisms with friction compensation. *Industrial Electronics, IEEE Transactions on*, 61(1):486–494, Jan 2014.
12. Sebastião Cícero Pinheiro Gomes and V Santos da Rosa. A new approach to compensate friction in robotic actuators. In *Proceedings IEEE International Conference on Robotics and Automation, 2003. ICRA'03.*, volume 1, pages 622–627. IEEE, 2003.
13. Silvio Traversaro, Andrea Del Prete, Riccardo Muradore, Lorenzo Natale, and Francesco Nori. Inertial parameter identification including friction and motor dynamics. In *IEEE-RAS International Conference on Humanoid Robots (Humanoid13), Atlanta, USA*, 2013.
14. Ren C Luo, CY Yi, and Yi W Perng. Gravity compensation and compliance based force control for auxiliarily easiness in manipulating robot arm. In *2011 8th Asian Control Conference (ASCC)*, pages 1193–1198. IEEE, 2011.
15. Chae H An, Christopher G Atkeson, and John M Hollerbach. *Model-based control of a robot manipulator*, volume 214. MIT press Cambridge, MA, 1988.
16. Ming Liu and Nghe H Quach. Estimation and compensation of gravity and friction forces for robot arms: Theory and experiments. *Journal of Intelligent and Robotic Systems*, 31(4):339–354, 2001.

17. Lorenzo Sciavicco and Luigi Villani. *Robotics: modelling, planning and control*. Springer, 2009.
18. Alessandro De Luca and Stefano Panzieri. Learning gravity compensation in robots: Rigid arms, elastic joints, flexible links. *International journal of adaptive control and signal processing*, 7(5):417–433, 1993.
19. Ivan Virgala and Michal Kelemen. Experimental friction identification of a dc motor. *International Journal of Mechanics and Applications*, 3(1):26–30, 2013.
20. S Martínez, CA Monje, Alberto Jardón, Paolo Pierro, Carlos Balaguer, and D Muñoz. Teo: Full-size humanoid robot design powered by a fuel cell system. *Cybernetics and Systems*, 43(3):163–180, 2012.
21. Niels Mallon, Nathan van de Wouw, Devi Putra, and Henk Nijmeijer. Friction compensation in a controlled one-link robot using a reduced-order observer. *IEEE Transactions on Control Systems Technology*, 14(2):374–383, 2006.
22. Santiago Morante, Juan G Victores, Santiago Martinez, and Carlos Balaguer. Sensorless friction and gravity compensation. In *Humanoid Robots (Humanoids), 2014 14th IEEE-RAS International Conference on*, pages 265–265. IEEE, 2014.